

**RADIOIMMUNOTHERAPY WITH  $^{213}\text{Bi}$  SYNERGIZES WITH PREDNISOLONE AND FLUDARABINE IN INDUCING APOPTOSIS IN B-CLL IN VITRO**

F. De Vos<sup>2</sup>, K. Vandenbulcke<sup>1</sup>, T. K. Nikula<sup>3</sup>, C. Apostolides<sup>3</sup>, R. Molinet<sup>3</sup>, H. Thierens<sup>1</sup>, R.A. Dierckx<sup>2</sup>, G. Slegers<sup>1</sup>, J. Philippe<sup>2</sup>, Fritz Offner<sup>2</sup>

1Ghent University, B-9000 gent, Belgium

2Ghent University Hospital, De Pintelaan 185, B-9000 Gent, Belgium

3ITU, Institut fur transuran chemie, Karlsruhe, Germany

Keywords:  $^{213}\text{Bi}$ , Rituximab, immunotherapy

To demonstrate that radio-immunotherapy is more effective than the combination of the cold antibody with an equal absorbed dose of gamma radiation we compared gamma irradiation of B-CLL cells in vitro with an alpha-emitter conjugated to an membranous (CD20) and an internalized antibody (CD19). In a previous study alpha-RIT with  $^{213}\text{Bi}$ -Rituximab was indeed shown to induce apoptosis in vitro in CLL cells more effectively than gamma plus cold antibody (RBE=2.2) in patients who were sensitive to chlorambucil, but not significantly in those who had become resistant to alkylator or fludarabine chemotherapy. To measure if the response initiated by alpha-RIT can be amplified or restored by radiosensitizers or agents that cripple antiapoptotic defenses induced or present in tumor cells, we combined this with fludarabine and/or corticosteroids .

$^{213}\text{Bi}$  was eluted from an 225-Ac generator and used conjugated to anti-CD20 or anti-CD19 with CHX-A"-DTPA as a chelator. B-CLL cells from 32 patients were cultured for 24 hours in CRPMI/10%FCS while exposed to the following treatments : (1)  $^{213}\text{Bi}$  conjugated anti-CD20(2Gy) (2)  $^{213}\text{Bi}$  conjugated anti-CD19(2Gy) (3) external 60-Co gamma-irradiation (2Gy), (4) Fludarabine 5 mM, (5) methylprednisolone 10  $\mu\text{M}$ , (6)  $^{213}\text{Bi}$  antiCD19 and 20 plus prednisolone and/or fludarabine (7) gamma radiation plus prednisolone and/or fludarabine. Apoptosis was scored by flowcytometry staining with AnnexinV-FITC and 7-AAD. The apoptosis score was expressed as % excess over spontaneous apoptosis in control culture medium.  $^{213}\text{Bi}$ -Rituximab alone induced significantly more apoptosis than external gamma radiation (24.5+14.8 % vs 17+11.5%,  $p < 0.001$ )  $^{213}\text{Bi}$ -antiCD-19 was superior to  $^{213}\text{Bi}$ -Rituximab with borderline statistical significance (32.7+17.8%,  $p=0.048$ , paired t). Treatment with prednisolone gave 22.6+13.2% and combination with  $^{213}\text{Bi}$ antiCD20, CD19 or gamma increased this to 46+13.9, 51.6+16.9 and 40.1+14.9% respectively. Fludarabine alone resulted in 13.4+ 12.7 and in combination with  $^{213}\text{Bi}$ antiCD20, CD19 or gamma this increased to 39.9+15.8, 46.6+19 and 30.7+18.1%. When combining fludarabine and prednisolone apoptosis was induced in 31.1+15.9 % of cells and addition of  $^{213}\text{Bi}$ antiCD20, CD19 or gamma increased this to 51.6+16.9, 55.9+17.2 and 44.9+16.7% respectively.

In conclusion, both fludarabine and corticosteroids were at least additive in inducing apoptosis when combined with gamma radiation or alpha-radioimmunotherapy of B-CLL in vitro.

## SELECTIVE TUMOUR LOCALISATION OF THE BONE-SEEKING RADIOPHARMACEUTICAL $^{117m}\text{Sn(II)}$ -PEI-MP AS STUDIED IN OSTEOSARCOMA CONTAINING MICE

J.R. Zeevaart<sup>1</sup>, W.K.A. Louw<sup>1</sup>, J.M. Wagener<sup>1</sup>, M.F. Botelho<sup>2</sup>, C. Gomes<sup>2</sup>, L. Metello<sup>2</sup>, A. Abrunhosa<sup>2</sup>, Z.I. Kolar<sup>3</sup>, I.C. Dormehl<sup>4</sup>

<sup>1</sup>Radiochemistry, NECSA, PO Box 582, Pretoria,0001, South Africa, radchem@aec.co.za, <sup>2</sup>Biophysics Department, IBILI, Faculty of Medicine, University of Coimbra, Portugal, <sup>3</sup>Radiochemistry, Interfaculty Reactor Institute, Delft University of Technology, Mekelweg 15, 2629 JB Delft, The Netherlands, <sup>4</sup>AEC Institute for Lifesciences, University of Pretoria, PO Box 2034, Pretoria 0001, South Africa

Key Words:  $^{117m}\text{Sn}$ , polymer, selective uptake, osteosarcoma tumour, mice

In the search for a cure for metastatic bone cancer,  $^{117m}\text{Sn}$  with its conversion electrons of discrete energies shows little bone marrow toxicity, providing the opportunity to increase the administered dose. Selective accumulation in lesions would capitalise on this advantage. The 10-30 kDa fraction of the water-soluble polymer polyethyleneimine, functionalised with methylene phosphonate groups (PEI-MP) (Fig. 1) and labelled with  $^{99m}\text{Tc}$ , has proved a promising agent for selective uptake into bone tumours<sup>1</sup>. From speciation calculations using the ECCLES database it was predicted<sup>2</sup> that Sn(II) will stay bound to the polymer in blood plasma and therefore should deliver the therapeutic radionuclide  $^{117m}\text{Sn(II)}$  to the bone with only a slight reticuloendothelial uptake. As this was the first blood plasma model that has been compiled for Sn<sup>II</sup>, predictions about the behaviour of  $^{117m}\text{Sn(II)}$ -PEI-MP in blood plasma were verified with primate tests<sup>3</sup>. The biodistribution studies on these healthy animals confirmed these predictions. To test the tumour selectiveness, tests in nude balb C mice containing canine osteosarcomas were carried out. Preliminary results (Table 2) indicated a highest tumour to background ratio of 14:1 after 60 minutes that decreases to ~6:1 after 210 minutes.

Table 1. Tumour to background ratio with time

Time	Tumour/Background
30 min	8.9
60 min	14.4
90 min	9.8
120 min	6.9
180 min	8.5
210 min	5.7

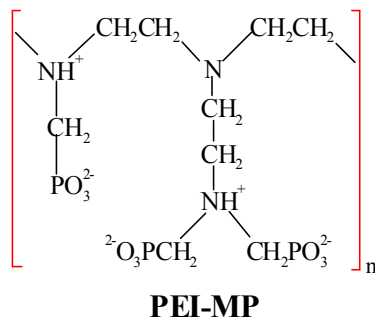


Fig. 1. Structure of the polymer, PEI-MP

### References:

1. I.C. Dormehl et al, *Drug Res.*, **51** (1), 258-263 (2001)
2. J.R. Zeevaart et al., *J. Radioanal. Nucl. Chem.*, **258** (2003) *in press*.
3. J.R. Zeevaart et al., *Drug Res.*, *Submitted*.

**SELECTIVE *IN VITRO* AND *IN VIVO* TARGETING OF HUMAN *E. COLI* ST PEPTIDE ANALOGS TO HUMAN PANCREATIC CANCER CELLS**

M. F. Giblin<sup>2</sup>, G. L. Sieckman<sup>1</sup>, H. Gal<sup>2</sup>, N. K. Owen<sup>2</sup>, T. J. Hoffman<sup>1,2</sup>, L. R. Forte<sup>1,2</sup>, W. A. Volkert<sup>1,2,3</sup>

<sup>1</sup>Harry S. Truman Memorial Veterans Administration Hospital, 800 Hospital Dr., Columbia, MO 65201, USA.

<sup>2</sup>University of Missouri-Columbia, Columbia, MO 65211. <sup>3</sup>volkertw@health.missouri.edu

**KEYWORDS:** Pancreatic cancer, Human *E. coli* ST peptide, guanylin, Indium-111

The human *E. coli* ST peptide (ST<sub>h</sub>, amino acid sequence N<sup>1</sup>SSNYCCCLCCNPACTGCY<sup>19</sup>) binds specifically to the Guanylate Cyclase C (GC-C) receptor, which is present in high density on the apical surface of normal intestinal epithelial cells as well as on the surface of human colon cancer cells. GC-C is the cognate receptor for the endogenous peptides guanylin and uroguanylin, which act to regulate ion and fluid homeostasis via activation of cGMP production in the intestine. Analogs of ST<sub>h</sub> are currently being used as vectors targeting human colon cancers. The aim of these studies is to demonstrate that ST<sub>h</sub> analogs with appended DOTA chelating moieties can also be specifically targeted to human pancreatic cancer cell types both *in vitro* and *in vivo*. Recent results in our laboratory have shown that ST<sub>h</sub> will bind with high affinity to an as yet unidentified receptor on the surface of human pancreatic cancer cells, including the CFPAC-1 cell line. Preliminary characterization of this receptor indicates that equilibrium binding of ST<sub>h</sub> to CFPAC-1 human pancreatic cancer cells occurs after 1 hr at 37°C, as is the case with GC-C expressing T84 human colon cancer cell lines. However, binding of ST<sub>h</sub> to CFPAC-1 cells does not elicit production of cyclic GMP as does ST<sub>h</sub> binding to GC-C on T84 cells. SDS-PAGE followed by <sup>125</sup>I-F<sup>19</sup>-ST<sub>h</sub>(1-19) autoradiography suggests that the unidentified receptor has an apparent molecular weight of 120-130 kDa, while GC-C migrates as a band of 150-160 kDa. Further distinguishing characteristics of the receptor present on human pancreatic cells are that it possesses a differing ligand specificity profile with respect to the GC-C ligands guanylin and uroguanylin, and that receptor internalization is diminished with respect to internalization of GC-C.

ST<sub>h</sub> analogs have been synthesized with pendant N-terminal DOTA moieties and radiolabeled with indium-111. ST<sub>h</sub> analogs were produced by SPPS using standard fmoc chemistry. Reduced, linear peptides were oxidatively refolded by stirring a 0.1 mg/ml peptide solution in 0.1 M ammonium formate, pH 8.0 at room temperature for periods up to 5 days. Refolded peptides were purified by C18 RP-HPLC and characterized by ESI-MS (DOTA-F<sup>19</sup>-ST<sub>h</sub>(1-19) calc m/z [M+H]<sup>+</sup>: 2411.8; found: 2410.6; DOTA-Q<sup>8</sup>, F<sup>19</sup>-ST<sub>h</sub>(1-19) calc m/z [M+H]<sup>+</sup>: 2410.8; found: 2411.3; DOTA-A<sup>6,7,10,11,15,18</sup>, F<sup>19</sup>-ST<sub>h</sub>(1-19) calc m/z [M+H]<sup>+</sup>: 2227.2; found: 2227.3). Additionally, the DOTA-F<sup>19</sup>-ST<sub>h</sub>(1-19) analog was produced using an orthogonal deprotection scheme in which pairs of free cysteine residues were sequentially deprotected and oxidized using Trt, AcM, and tBu thiol protecting groups. Both oxidative refolding and orthogonal deprotection produced identical products as assessed by RP-HPLC retention time, ESI-MS, and receptor binding assay. <sup>111</sup>In conjugates were prepared in high yield (>95% RCP) by addition of <sup>111</sup>InCl<sub>3</sub> in 0.05 M HCl (7.4-74 MBq) to a solution of DOTA-peptide (50 g) in 200 l 0.4 M ammonium acetate, pH 6.0. Reaction mixtures were incubated for 1 hr at 80°C, quenched by addition of 50 l 2 mM EDTA, and purified by C18 RP-HPLC.

*In vitro* competitive binding assays employing CFPAC-1 human pancreatic cancer cells demonstrated an IC<sub>50</sub> value of 9.2 ± 2.1 nM for the DOTA-F<sup>19</sup>-ST<sub>h</sub>(1-19) analog and a fivefold lower IC<sub>50</sub> for an analog with an E to Q point mutation at position 8. An analog lacking tertiary structure by virtue of alanine substitutions at all six positions containing cysteine in the wild-type molecule showed no displacement in the assay. *In vivo* pharmacokinetic studies in CFPAC-1 human pancreatic cancer derived xenografts in SCID mice demonstrate moderate specific tumor uptake of 0.59 ± 0.2 %ID/g at 1 hr pi for the <sup>111</sup>In-DOTA-F<sup>19</sup>-ST<sub>h</sub>(1-19) analog, with 0.12 ± 0.07 %ID/g in the pancreas. These results suggest that radiolabeled ST<sub>h</sub> analogs could hold potential as agents for the imaging and treatment of human pancreatic cancers.

**<sup>64</sup>Cu LABELING AND EVALUATION OF THE METALLOPEPTIDE, DOTA-ReCCMSH(Arg<sup>11</sup>), A CYCLIZED α-MSH ANALOGUE**P. McQuade<sup>1</sup>, J.S. Lewis<sup>1</sup>, T.P. Quinn<sup>2</sup> and M. J. Welch<sup>1</sup><sup>1</sup>Mallinckrodt Institute of Radiology, Washington University School of Medicine, St. Louis, MO 63110.<sup>2</sup>Department of Biochemistry, University of Missouri-Columbia, Columbia, MO 65212. *Contact:* Paul McQuade, Mallinckrodt Institute of Radiology, Washington University School of Medicine, Campus Box 8225, 510 S. Kingshighway Blvd. Saint Louis, MO 63110, USA. Email: mcquadep@mir.wustl.edu

Keywords: melanoma, copper-64, metallopeptide, microPET imaging

Recently the rise in occurrence of malignant melanoma in Europe and America has become cause for concern.(1-2) The early detection of these malignant melanoma has proved difficulty and so efforts for the development of new agents is essential. Some of the most promising agents examined to-date are peptide analogues of the alpha-melanocyte stimulating hormone, α-MSH.(1-2) Previous studies on α-MSH analogues showed that the rhenium-cyclized peptide <sup>188</sup>ReCCMSH, exhibited high tumor uptake and rapid clearance from normal organs, in both murine and human melanoma models.(3) The DOTA bifunctional chelator was then attached, but it was found that this resulted in elevated kidney uptake. <sup>111</sup>In studies showed however that replacing the lysine residue present in ReCCMSH with an arginine residue caused a reduction in renal uptake.(2) The goal was to carry out studies with <sup>64</sup>Cu labeled DOTA-ReCCMSH(Arg<sup>11</sup>) to determine if it is a viable agent for the detection of malignant melanoma, via PET imaging.

The labeling of DOTA-ReCCMSH(Arg<sup>11</sup>) with <sup>64</sup>Cu takes place at 65°C for 1 hr, and the reaction mixture is then purified by RP-HPLC. Utilizing this method, radiolabeling yields of <sup>64</sup>Cu-DOTA-ReCCMSH(Arg<sup>11</sup>) of up to 60% have been achieved. Rodent biodistribution at 30 min, 2, 4 and 24 h have been obtained with <sup>64</sup>Cu-DOTA-ReCCMSH. In these experiments C57 mice bearing B16/F1 murine melanoma tumors were injected with <sup>64</sup>Cu-DOTA-ReCCMSH. After administering the radiopharmaceutical the mice were sacrificed at the desired time point and the organs harvested and taken for scintillation well-counting. Tumor uptake reached a maximum 4 hr post-injection and gradually decreased over 24 hours. The values obtained were lower than those reported for <sup>111</sup>In-DOTA-ReCCMSH. Another difference in distribution between <sup>64</sup>Cu-DOTA-ReCCMSH and <sup>111</sup>In-DOTA-ReCCMSH was observed in the liver. Liver uptake of the <sup>111</sup>In complex reaches a maximum after 30 minutes (0.66 ± 0.05 %ID/g) and slowly decreased over 24 hr (0.32 ± 0.09 %ID/g). The liver uptake of the <sup>64</sup>Cu labeled complex however reached its maximum after 2 hr (9.68 ± 1.71 %ID/g) and reduced only slightly after 24 hr (6.23 ± 1.31 %ID/g). This increase in liver uptake is primarily due to decomposition and transchelation of <sup>64</sup>Cu-DOTA in the liver, and is likely to be reduced by the use of a more stable macrocyclic conjugate. MicroPET images of <sup>64</sup>Cu-DOTA-ReCCMSH(Arg<sup>11</sup>) have also been obtained with C57 mice bearing B16/F1 murine melanoma tumors. In these studies the tumor can be easily be visualized after 2 hr. MicroPET images also show that the administering of a blocking dose, by saturating the α-MSH receptor binding sites, substantially reduces tumor uptake. The data obtained suggests that this Cu-melanoma agent has the potential for early detection of malignant melanoma by exploiting the sensitivity and high resolution of PET.

This work and the production of <sup>64</sup>Cu was financially supported by the National Cancer Institute (1 R24 CA86307). MicroPET imaging is supported by an NIH/NCI SAIRP grant (1 R24 CA83060) with additional support from the Small Animal Imaging Core of the Alvin J. Siteman Cancer Center at Washington University and Barnes-Jewish Hospital. The SAIC Core is supported by an NCI Cancer Center Support Grant # 1 P30 CA91842.

1. Miao Y, Owen NK, Hoffman TJ, *et al.* *Technetium, Rhenium and Other Metals in Chemistry and Nuclear Medicine* 2002; 6: 375-380
2. Cheng Z, Chen J, Miao Y, *et al.* *J. Med. Chem.* 2002; 45: 3048-3056
3. Giblin MF, Wang N, Hoffman TJ, *et al.* *Proc. Natl. Acad. Sci.* 1998; 95: 12814-12818

## MICROPET IMAGING OF A TITANIUM-45 LABELED TITANOCENE COMPLEX TO DELINEATE BIODISTRIBUTION OF TITANIUM ANTI-CANCER DRUGS

A. L. Vavere<sup>1,2</sup> and M. J. Welch<sup>1,2</sup>

<sup>1</sup>Department of Chemistry, Washington University in St. Louis, MO, 63130, USA <sup>2</sup>Division of Radiological Sciences, Washington University School of Medicine, St. Louis, MO, 63110, USA. Email: VavereA@mir.wustl.edu

Keywords: titanium-45, transferrin, titanocene dichloride, microPET

Titanium(IV) complexes have been shown to exhibit high antitumor activity against a range of tumors with less toxic side effects than cisplatin (1). One compound currently in clinical trials for cancer, titanocene dichloride, has been extensively studied to elucidate its mechanism of action. Interestingly, the compound is prepared clinically in a virtually aqueous solution in which the compound is known to rapidly hydrolyze (2). Titanium(IV) from titanocene dichloride is readily taken up by transferrin under physiological conditions (3). The same group reported that Ti(IV) binds strongly to transferrin suggesting that it may mediate the uptake of Ti from anticancer drugs into cells (4).

Titanium-45 has a half-life of 3.08 hours and decays 85% by positron emission with  $E_{+max} = 1.04$  MeV. Published work on the application of titanium radiopharmaceuticals has been limited, but <sup>45</sup>Ti has been explored as a potential metal for labeling pharmaceuticals for PET imaging by forming complexes with DTPA, citric acid, and human serum albumin (5). It was previously reported by our group that <sup>45</sup>Ti-transferrin targets tumor tissue with visual intensity of 60% higher than that of non-target tissue by microPET (6). The aim of this study was to synthesize a derivative of titanocene dichloride using radionuclidic techniques and compare its biodistribution to that of <sup>45</sup>Ti-transferrin.

Titanium-45 was produced using a method similar to that of Ishiwata *et al.* (5). Titanocene dichloride was successfully synthesized by combining TiCl<sub>4</sub> and sodium cyclopentadienide in THF under a nitrogen atmosphere following a small-scale adaptation of a published procedure (7). This procedure was then adjusted to include the presence of <sup>45</sup>Ti by doping TiCl<sub>4</sub> with <sup>45</sup>Ti prior to initiation of the reaction. The compound was prepared for experiments without further purification in 10% DMSO/saline resulting in a yellow solution, indicative of a Ti-OH species. Reverse-phase radio-HPLC using a 10% acetonitrile:water eluent shows effective labeling of one of the two resulting products. Full characterization of the final species is currently underway.

Female BALB/c mice were implanted with EMT-6 mammary carcinoma tumor cells subcutaneously and the tumors were given 7-12 days to grow. Static microPET imaging was performed at 2 and 4 hours post injection. Preliminary results show virtually identical organ uptake between the <sup>45</sup>Ti-transferrin and <sup>45</sup>Ti-titanocene derivative. This suggests a decomposition of the titanocene complex and similar delivery as that of <sup>45</sup>Ti-transferrin.

We are grateful for financial support from the Department of Energy (DE FG02 84ER60218 [M.J.W.]). MicroPET imaging was supported by an NIH/NCI SAIRP grant (1 R24 CA83060) and the Small Animal Imaging Core of the Alvin J. Siteman Cancer (NCI Cancer Center Support Grant # 1 P30 CA91842).

1. Kopf-Maier P, Kopf H. *Metal Compounds in Cancer Therapy*, Chapman & Hall: London, 1994.

2. Toney J H, Marks T J. *J Am Chem Soc* 1985; 107: 947-953.

3. Guo M, Sun H, McArdle H J *et al. Biochem* 2000; 39: 1023-1033.

4. Sun H, Li H, Weir R A, Sadler P J. *Angew Chem Int Ed* 1998; 37: 1577-1579.

5. Ishiwata K, Ito T, Monma M *et al. Appl Radiat Isot* 1991; 42: 707-712.

6. Vavere A L, Jones L A, McCarthy T J *et al. J Label Compd Radiopharm* 2001; 44: 793-795.

7. Wilkinson G, Birmingham J M. *J Am Chem Soc* 1954; 74: 4281-4284.

**COMPARISON OF THE IN VIVO DISTRIBUTIONS OF AN ANTIBODY FAB' LABELED BY CONJUGATION OF N-SUCCINIMIDYL *PARA*-[<sup>211</sup>AT]ASTATOBEZOATE AND BY DIRECT <sup>211</sup>AT LABELING USING PRECONJUGATED *NIDO*-CARBORANES, AND A *CLOSO*-DECABORANE**

D.S. Wilbur<sup>1</sup>, D.K. Hamlin<sup>1</sup>, M.-K. Chyan<sup>1</sup>, J. Quinn<sup>2</sup>, R.L. Vessella<sup>2</sup>, T.J. Wedge<sup>3</sup>, and M.F. Hawthorne<sup>3</sup>

<sup>1</sup>Departments of Radiation Oncology, University of Washington, 2121 N. 35<sup>th</sup> St., Seattle, WA 98103-9103

<sup>2</sup>Department of Urology, University of Washington, Seattle, WA

<sup>3</sup>Department of Biochemistry and Chemistry, University of California, Los Angeles, dswilbur@u.washington.edu

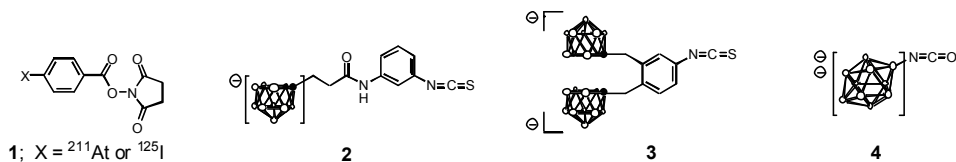
Keywords: astatine-211, protein labeling, *nido*-carboranes, decaborane

An investigation was conducted to compare the labeling yields and in vivo distributions of a monoclonal antibody Fab' fragment astatinated by using four different conjugates (**1-4**). Fab' was used in the investigation as previous studies comparing Fab' conjugated with [<sup>211</sup>At]**1** had shown that the label was unstable towards in vivo deastatination. Thus, the primary objective of the study was to evaluate the in vivo stability of the astatinated Fab' conjugates. Additionally, the (non-optimized) labeling yields obtained with each conjugate were compared, and a determination of whether the labeling method altered the in vivo distribution of the protein was made.

The labeling experiments were conducted with anti-PSMA monoclonal antibody 107-1A4 Fab' fragment (N-ethyl maleimide capped). Preparation and conjugation of [<sup>211</sup>At]**1** with the Fab' gave an overall radiochemical yield of 14%. Fab' was conjugated separately with *nido*-carboranyl derivative **2**, a bis-*nido*-carboranyl derivative (Venus Flytrap Complex) **3**, and a decaborane derivative **4**. Radiolabeling of Fab' preconjugated with **2**, **3** or **4** using Chloramine-T (ChT)/Na[<sup>211</sup>At]At gave radiochemical yields of 28%, 32%, and 36%, respectively. Importantly, direct astatination of native Fab' employing the same conditions gave <1% radiochemical yield. Size-exclusion HPLC of the Fab' conjugated with **1** or **4** displayed peaks that were similar to the native Fab', whereas Fab' conjugated with **2** or **3** displayed very broad HPLC peaks.

Biodistribution studies of dual labeled (<sup>211</sup>At and <sup>125</sup>I) Fab' conjugated with **1**, **2**, **3**, or **4** were conducted in athymic mice at 1 and 4h post injection (pi). The <sup>211</sup>At stability on Fab' conjugated with [<sup>211</sup>At]**1** was low based on the differences in radionuclides observed in the spleen (10.5 %ID/g <sup>211</sup>At vs. 1.7 %ID/g <sup>125</sup>I) and lung (11.7 %ID/g <sup>211</sup>At vs 4.3 %ID/g <sup>125</sup>I) at 4h pi. Contrary to that, the stability of <sup>211</sup>At-labeled Fab' conjugated with **2**, **3**, or **4** appeared quite high as only small differences were observed in spleen and lung. To determine the effect of the conjugate employed, the distributions of radiolabeled Fab' conjugates were compared with Fab' conjugated with [<sup>125</sup>I]**1**. Radiolabeled Fab' conjugated with **4** had a biodistribution that was most similar to Fab' conjugated with [<sup>125</sup>I]**1**. For example, Fab' conjugated with **4** or **1** had high kidney concentrations (<sup>211</sup>At: 29.6 %ID/g vs. 30.9 %ID/g resp. at 4h pi) as expected for a Fab' fragment, while conjugates of **2** and **3** were considerably lower (<sup>211</sup>At: 12.0 %ID/g & 3.7 % ID/g, resp.). Additionally, Fab' conjugated with **2** remained in the blood (<sup>211</sup>At: 19.1 %ID/g at 4 h pi), whereas Fab' conjugated with **3** had lower blood concentration (<sup>211</sup>At: 6.6 %ID/g), but high spleen and liver concentrations.

The results indicate the Fab' conjugated with **4** labels directly with <sup>211</sup>At in fair yields, is stable to in vivo deastatination, and has a minimal effect on the protein's distribution. Therefore, it is a good candidate for further studies involving astatination of proteins and other biomolecules.



(Note: solid circles in borane structures represent C or CH and open circles represent B or BH)

## A NEW GENERATION OF CARBOHYDRATED F-18-LABELLED SST-LIGANDS: FAST SYNTHESIS, HIGH YIELDS AND EXCELLENT PHARMACOKINETICS

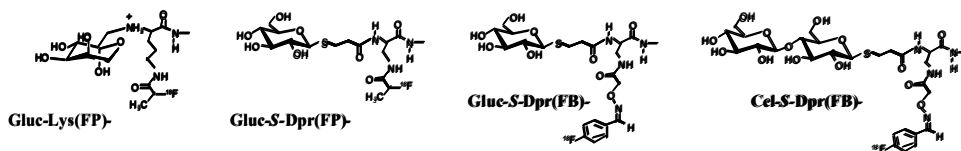
M. Schottelius, T. Poethko, M. Herz, M. Schwaiger, H.-J. Wester

Department of Nuclear Medicine, Klinikum rechts der Isar, Technical University of Munich, Ismaningerstr. 22, D-81675 Munich, Germany

Keywords: somatostatin, carbohydration, chemoselective ligation, F-18, PET

**Aims:** First PET studies in patients using N-(1-deoxy-D-fructosyl)-N-(2-[<sup>18</sup>F]fluoropropionyl)-Lys<sup>0</sup>-Tyr<sup>3</sup>-octreotate ([<sup>18</sup>F]Gluc-Lys(FP)-TOCA) have shown very promising results<sup>1</sup>. However, the time-consuming multistep synthesis and resulting low overall yields limit the applicability of this radioligand for clinical routine. Consequently, new carbohydrate octreotate (TOCA) derivatives were prepared via a chemoselective two-step <sup>18</sup>F-labelling strategy<sup>2</sup> (oxime ligation) and compared to their corresponding analogs synthesized by <sup>18</sup>F-fluoropropionylation.

**Methods:** Fmoc-Lys<sup>0</sup>(Boc)- and Fmoc/Boc-Dpr<sup>0</sup>(Boc/Fmoc)-Tyr<sup>3</sup>-Lys<sup>5</sup>(Dde)-TOCA were synthesized using Fmoc-chemistry. N-terminal glycosylation was performed via Amadori reaction with glucose or coupling with peracetylated 1-mercaptopropionyl-glucose (Gluc-S-) or -cellobiose (Cel-S-). The aminoxy-functionality for <sup>18</sup>F-fluorination via oxime bond formation was introduced by coupling (Boc)oxyaminoacetic acid to the Dpr<sup>0</sup>-sidechain, followed by complete deprotection. Reaction with 4-[<sup>18</sup>F]fluorobenzaldehyde (FB) afforded Gluc-S-/Cel-S-Dpr[(4-[<sup>18</sup>F]fluorophenyl)oximeacetyl]-TOCA ([<sup>18</sup>F]Gluc/Cel-S-Dpr(FB)-TOCA) in 65-75% radiochemical yield (based on FB). For <sup>18</sup>F-fluoroacylation, Lys<sup>5</sup>(Dde)-protected precursors were reacted with 4-nitrophenyl 2-[<sup>18</sup>F]fluoropropionate (FP) and then deprotected, yielding [<sup>18</sup>F]Gluc-Lys(FP)- and [<sup>18</sup>F]Gluc-S-Dpr(FP)-TOCA in 25-70% RCY (based on FP). Biodistribution studies 10 min and 1 h p.i. (n = 5) were carried out using AR42J tumor bearing nude mice. For competition experiments (n = 3), 15 µg of cold Tyr<sup>3</sup>-octreotide were coinjected.



**Results:** Only [<sup>18</sup>F]Gluc-S-Dpr(FB)-TOCA (logP<sub>ow</sub> = -1.24 ± 0.03) shows considerable uptake in liver and intestine (1 h p.i.: 3.5 ± 0.9 and 7.0 ± 1.2 %iD/g, respectively). While for [<sup>18</sup>F]Gluc-Lys(FP)-TOCA and [<sup>18</sup>F]Cel-S-Dpr(FB)-TOCA (identical logP<sub>ow</sub> = -1.70 ± 0.03) accumulation in these organs at 1 h p.i. is reduced by a factor of 4-5, kidney uptake of the three compounds is comparable (7.5-8.7 %iD/g). In contrast, [<sup>18</sup>F]Gluc-S-Dpr(FP)-TOCA (logP<sub>ow</sub> = -2.80 ± 0.01) shows very low accumulation in all excretion organs (liver: 0.2 ± 0.04, intestine: 1.1 ± 0.1, kidney: 1.9 ± 0.7 %iD/g at 1 h p.i.). All compounds investigated show high and specific uptake in all sst-positive tissues. While tumor accumulation 1 h p.i. was comparable both for the two FP- (13.5-15.1 %iD/g) and for the two FB-analogs (21.8-24.0 %iD/g), tumor/organ ratios were highest for [<sup>18</sup>F]Gluc-S-Dpr(FP)-TOCA (t/blood: 122 ± 34, t/liver: 66 ± 15, t/intestine: 14 ± 2, t/kidney: 8 ± 3) and [<sup>18</sup>F]Cel-S-Dpr(FB)-TOCA (t/blood: 42 ± 8, t/liver: 27 ± 5, t/intestine: 15 ± 2, t/kidney: 3.2 ± 0.4).

**Conclusion:** [<sup>18</sup>F]Cel-S-Dpr(FB)-TOCA shows high tumor/non-tumor ratios and excellent excretion properties. [<sup>18</sup>F]Cel-S-Dpr(FB)-TOCA can be synthesized in high yields (overall 50% RCY) by chemoselective ligation of the unprotected peptide using [<sup>18</sup>F]fluorobenzaldehyde. Thus, [<sup>18</sup>F]Cel-S-Dpr(FB)-TOCA is an extremely promising tracer for sst-imaging with PET.

<sup>1</sup> H.J. Wester, M. Schottelius, K. Scheidhauer, G. Meisetschläger, M. Herz, F. Rau, J.C. Reubi, M. Schwaiger. *Eur. J. Nucl. Med.* **2003**, *30*, 117-122

<sup>2</sup> T. Poethko, G. Thumshirn, U. Hersel, M. Schottelius, G. Henriksen, M. Herz, H. Kessler, M. Schwaiger, H.J. Wester. see abstract in this volume

## SYNTHESIS OF TECHNETIUM-99m LABELED GLUCOSAMINO-Asp-Lys-Arg-Gly-Asp-D-Phe AS A POTENTIAL TUMOR IMAGING AGENT

B.C. Lee,<sup>1</sup> H.J. Sung,<sup>1</sup> S.H. Song,<sup>2</sup> Y.S. Choe,<sup>2</sup> K.-H. Lee,<sup>2</sup> K.-H. Chung,<sup>1</sup> D.Y. Chi,<sup>1</sup>

<sup>1</sup>Department of Chemistry, Inha University, 253 Yonghyundong Namgu, Incheon 402-751, Korea,

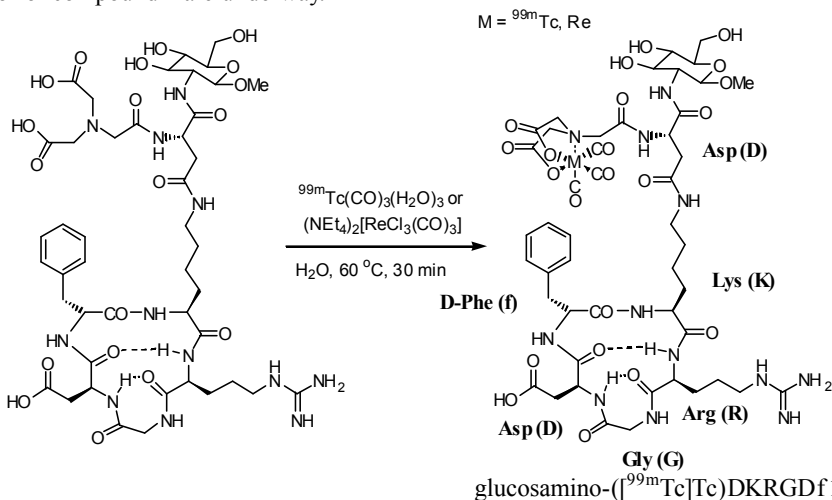
<sup>2</sup>Department of Nuclear Medicine, Samsung Medical Center, Sungkyunkwan University School of Medicine, 50 Ilwon-dong, Kangnam-ku, Seoul 135-230 Korea. E-mail: dychi@inha.ac.kr

Keywords:  $\alpha_3$  Integrin, Integrin binding peptide, RGD, <sup>99m</sup>Tc, Tumor imaging

As the  $\alpha_3$  integrins is expressed on proliferating endothelial cells as well as on tumor cells of various origin, tumor-induced angiogenesis could be blocked by antagonizing the  $\alpha_3$  integrins with RGD. Therefore, many groups investigated RGD glycopeptides as  $\alpha_3$  integrins antagonists and labeled with iodine-123 and fluorine-18. Recently, Janssen *et al.* reported the in vivo behavior of the radiolabeled dimeric RGD peptide E-[c(RGDfK)]<sub>2</sub>, conjugated with 1,4,7,10-tetraazadodecane-N,N',N'',N'''-tetraacetic acid (DOTA) or hydrazinonicotinamide (HYNIC) and chelated with <sup>111</sup>In, <sup>90</sup>Y, or <sup>99m</sup>Tc, in the NIH:OVCAR-3 s.c. ovarian carcinoma xenograft model in BALB/c nude mice [1].

With our another development of fluorine-18 labeled RGD glycopeptide (glucosamino-([<sup>18</sup>F]fluorobenzyl)DKRGDf), we designed technetium-99m labeled RGD glycopeptide – glucosamino-([<sup>99m</sup>Tc]Tc)-Asp-Lys-Arg-Gly-Asp-D-Phe (glucosamino-([<sup>99m</sup>Tc]Tc)DKRGDf **1**) as a diagnostic tumor imaging agent for SPECT. The target peptide was prepared using a solid support coupling protocol. The precursor was obtained by deprotection of tri-*O*-benzylglucosamino-*N*-[(bisbenzyloxycarbonylmethyl)amino-acetyl]-Asp-Lys-(*N*-pbf)-Arg-Gly-(*O*-*t*-butyl)Asp-D-Phe.

<sup>99m</sup>Tc(CO)<sub>3</sub> incorporation to the precursor was carried out in water at 60 °C for 30 min in 90-93% radiochemical yields and then purified by HPLC at a flow rate of 2 mL/min (0-50% CH<sub>3</sub>CN/0.1% TFA in H<sub>2</sub>O, 50 min). The desired fraction eluted at 29.8 min was collected and matched with cold compound (T<sub>R</sub> = 30.9 min). Optimization for labeling conditions and biological evaluation of compound **1** are underway.



Acknowledgement. We thank Mallinckrodt Inc., Nuclear Medicine R&D, Petten, The Netherlands for the generous gifts of the tricarbonyltechnetium kits.

1. Janssen ML, Oyen WJ, Dijkgraaf I, Massuger LF, Frielink C, Edwards DS, Rajopadhye M, Boonstra H, Corstens FH, Boerman OC. *Cancer Res* 2002;62:6146-6151.